Journal of Molecular Structure 1075 (2014) 196–203

Contents lists available at ScienceDirect

Journal of Molecular Structure

journal homepage: www.elsevier.com/locate/molstruc

Reinforcement of poly(amide–imide) containing N-trimellitylimido-L-phenylalanine by using nano α-Al_2O_3 surface-coupled with bromo-flame retardant under ultrasonic irradiation technique

Shadpour Mallakpour [a,b,c,*], Elham Khadem [a]

[a] Organic Polymer Chemistry Research Laboratory, Department of Chemistry, Isfahan University of Technology, Isfahan 84156-83111, Islamic Republic of Iran
[b] Nanotechnology and Advanced Materials Institute, Isfahan University of Technology, Isfahan 84156-83111, Islamic Republic of Iran
[c] Center of Excellence in Sensors and Green Chemistry, Department of Chemistry, Isfahan University of Technology, Isfahan 84156-83111, Islamic Republic of Iran

HIGHLIGHTS

- A straightforward and fast method was used for the surface modification of ANPs.
- Flame retardant THCB was utilized for the modification of ANPs.
- Modified ANP was improved the thermal properties of PANCs.
- TEM and FE-SEM images proved that ANPs were dispersed in the PAI matrix.

GRAPHICAL ABSTRACT

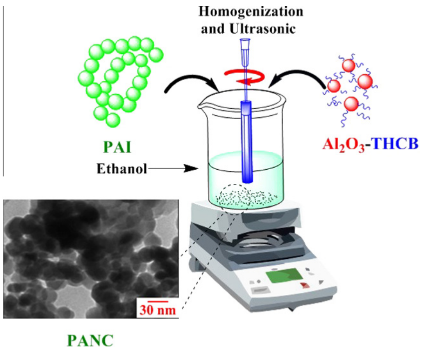

ARTICLE INFO

Article history:
Received 5 May 2014
Received in revised form 25 June 2014
Accepted 25 June 2014
Available online 2 July 2014

Keywords:
Nanocomposite
Surface modification
Flame retardant
Poly(amide–imide)
Thermogravimetric analysis (TGA)

ABSTRACT

By the uniform dispersion of nanoparticles into a polymer matrix, a substantial improvement of physicochemical properties can be attained. In this study, a series of poly(amide–imide)/Al_2O_3 nanocomposites (PANC)s based on various amounts of modified α-Al_2O_3 nanoparticles (ANP)s were prepared using the ultrasonic irradiation method. In the process of manufacturing the nanocomposites (NC)s, severe agglomeration of ANPs into the polymer matrix can be reduced using 2,3,4,5-tetrabromo-6-[(4-hydroxyphenyl)carbamoyl]benzoic acid as novel coupling agent. The effects of modified ANPs on the morphology and properties of the polymer matrix were studied by means of Fourier transform infrared spectroscopy, X-ray diffraction, field emission scanning electron microscopy, transmission electron microscopy and thermal gravimetric analysis (TGA). The results obtained by TGA showed that the thermal stability of the NCs was improved with the addition of the small amounts of ANPs as effective thermal degradation resistant reinforcement.

Introduction

Aromatic poly(amide–imide) (PAI) is one of the most class of alternative polymers with high strength and good solubility in polar amide-type solvents, which provide suitable accordance between processability and high thermal stability. They bring together both the advantages of polyamide and polyimide such

---

* Corresponding author at: Center of Excellence in Sensors and Green Chemistry, Department of Chemistry, Isfahan University of Technology, Isfahan 84156-83111, Islamic Republic of Iran. Tel.: +98 31 3391 3267; fax: +98 31 3391 2350.

E-mail addresses: mallak@cc.iut.ac.ir, mallak777@yahoo.com, mallakpour84@alumni.ufl.edu (S. Mallakpour).

http://dx.doi.org/10.1016/j.molstruc.2014.06.081
0022-2860/

as heat-resistant and good mechanical properties, easy processing and solvent resistance characteristic. Thus, they can be widely used in the numerous industries [1–3]. One of approaches to enhancement of the mechanical property, the thermal and chemical stability of PAI is the preparation of their composite ceramic materials [4].

The incorporation of an appropriate amount of nanosized material into the polymer matrix has gained significant physicochemical properties, which is not possible for conventional composites with micro or even macro scale fillers [5]. One well-known characteristics of nanoparticles (NP)s is the high specific surface area (total surface area of a material per unit of mass), which differentiates them from microparticles, and is essential for the enhancement of performance activity [6,7].

In nanocomposites (NC)s, strong chemical bonds (covalent or ionic) or interactions such as the van der Waals force, hydrogen bonding, or electrostatic force, often exist between the organic and inorganic components [8]. These interactions, not only caused the NPs fixated in the structure of NC, but also made large potential applications in the polymer hybrid [9,10].

Corundum aluminum oxide (α-Al_2O_3) is the most stable shape between the other phases, which is formed at the high temperature of about 1000 °C. This ceramic material, due to the superior properties such as high thermal conductivity, high hardness, high dielectric constant, good wear resistance, and catalyst can be widely used as reinforcer, in the polymer hybrids [11,12]. Nonetheless, intrinsically poor compatibility of most inorganic nanofillers with the organic polymer leads to poor dispersion and aggregation of NPs in the polymer matrix. Since, most of the NPs surface was covered with varying degrees of polar hydroxyl groups [13,14]. Hence, the pure NPs often discord in the hydrophobic matrix and can attract each other by interactions between the hydroxyl groups, and then form coagulum with size of several micrometers [15]. In order to alter the surface properties of the α-Al_2O_3 NPs (ANPs) and diminished intermolecular interaction, a number of functional groups and organic compounds, such as silane coupling agent [16,17], isocyanate group [18], stearic acid [19], dimethyl sulfoxide [20], acetic acid [21], have been used as modifying agents. The existence of the halogen and aromatic ring in coupling agents can act as flame retardant groups in NCs. However, the efficacy of halogenated flame retardants depends on the sort of halogen. Bromine and chlorine-based compounds, because of their weak bonding with carbon atoms, can be readily released and participate in the combustion process and so stopping the chain disintegration [22].

In the present study, we generally attempted to describe the synthesis and characterization of a series of chiral poly(amide–imide)/Al_2O_3 NCs (PANC) using a simple ultrasonically-assisted solution blending procedure. Therefore, ANPs are etched and modified with 2,3,4,5-tetrabromo-6-[(4-hydroxyphenyl)carbamoyl]benzoic acid, which is introduced the bulky substituent onto the surface of ANPs and is prevented agglomeration of ANPs in the host polymer. Organosoluble and thermally stable chiral PAI was synthesized during direct polymerization reaction of *N*-trimellitylimido-L-phenylalanine (DAPh) and 1,5-naphthalene diamine (NDA) under a medium consisting of molten tetra-butylammonium bromide (TBAB) and triphenyl phosphite (TPP). Then PANCs containing various ratios of the modified ANPs were synthesized under ultrasonically-assisted technique.

Experimental

Reagents and materials

ANP was purchased from Nanosabze Co. (Tehran, Iran), and size of the nanoalumina was 80 nm. TBAB, trimellitic anhydride (TMA) and NDA were purchased from Merck Co. and were used as received without further purification. *N*,*N*′-dimethylformamide (DMF) was dried over BaO and then distilled under the reduced pressure. Other chemicals used in this study were purchased from Fluka Chemical Co. (Buchs, Switzerland), Aldrich Chemical Co. (Milwaukee, WI), and Merck Chemical Co. (Germany).

Measurements

Melting points of the samples were measured on a melting point apparatus (Gallenhamp, England) without correction. A Jasco-680 Fourier transform-infrared (FT-IR) spectroscopy (Japan) was employed to examine the chemical bands on the polymer and PANCs. The spectra of solids were obtained using KBr pellets. The vibrational transition frequencies have been reported in wave numbers (cm^{-1}). The band intensities were assigned as weak (w), medium (m), strong (s), and broad (b). Thermal gravimetric analysis (TGA) is performed with a STA503 (Bahr-Thermoanalyse GmbH, Hüllhorst, Germany) at a heating rate of 20 °C min^{-1} from 25 to 800 °C under argon atmosphere. The X-ray diffraction (XRD) patterns were recorded using a Philips Xpert MPD diffractometer equipped with a Cu Kα anode ($\lambda = 0.151418$ nm) in 2θ range of 10–80° at the speed of 0.05° min^{-1}. The surface morphology of the samples was observed by field emission scanning electron microscopy (FE-SEM) (HITACHI S-4160, Japan). The dispersal of nano-fillers within the host matrix has been controlled by the transmission electron microscopy (TEM) (Philips CM 120) at an accelerating voltage of 150 kV. Preparation of PANC was carried out on a MISONIX ultrasonic XL-2000 SERIES (Raleigh, North Carolina, USA) with frequency 2.25 × 104 Hz and the power of 100 W.

THCB synthesis procedure

The amount of 0.10 g (0.22×10^{-3} mol) tetrabromophthalic anhydride (TBPA) and 0.02 g of (0.22×10^{-3} mol) *p*-aminophenol (PAP) were dissolved in acetone. The mixture was stirred for 4 h at room temperature. The resulting solution was poured in 20 mL of distilled water, the obtained precipitate was filtered and dried at 60 °C for 6 h under vacuum to give 0.103 g (83%) of white powder 2,3,4,5-tetrabromo-6-[(4-hydroxyphenyl)carbamoyl]benzoic acid (THCB). The purity of this compound was primarily checked with thin-layer chromatography (TLC) in a mixture of 80/20 of ethyl acetate/cyclohexane (m.p = 287–289 °C) [23].

Surface treatment of ANPs

Typical steps were carried out as follows: 15 wt.% of THCB was dissolved in 20 mL of ethanol at room temperature and 0.10 g of dried nano α-Al_2O_3 were added into it. This solution was vigorously stirred for 24 h and then, was ultrasonicated for 30 min. Finally, solution containing the ANPs was filtrated off and washed with ethanol three times. The solid was dried at 60 °C for 18 h. FT-IR peaks (KBr, cm^{-1}): $\bar{\nu} = 3500$–3300 (m, b, O—H and N—H stretching), 1700 (w, carboxylic acid's C=O), 1170 (w), 1266 (w), 1127 (w, stretching vibration of the C—O), 1400 (w, C—O—H deformation vibration).

Synthesis of diacid derived from amino acid

Optically active DAPh was prepared according to our previous work [24].

Polymer synthesis

PAI was synthesized by the direct polycondensation reaction of an equimolecular mixture of DAPh and NDA in a system of TBAB/TPP as condensing agent, which its procedure was reported in our preceding work [25].

Manufacture of PANCs

The 0.1 g of PAI was dispersed in 20 mL of absolute ethanol. A uniform suspension was obtained after sonication for 15 min. The appropriate amounts of modified ANPs (5, 10, 15 wt.%) were added in the PAI suspension with simultaneous stirring and then sonicated for 2 h. Finally, the solvent was removed and precipitated solid was dried in vacuum at 80 °C for 10 h.

Results and discussions

Synthesis of THCB

Fig. 1 shows the reaction between PAP and TBPA in acetone. In this reaction, the NH_2 group of PAP with more nucleophilic characteristic than phenolic OH attacked to the anhydride ring of TBPA and led to the formation of amic acid with three final functional groups, acid, amide and phenolic OH. The final product was precipitated in distilled water as a non-solvent. The presence of halogen atoms in the molecule can improve the efficiency of the fire retardant behavior. The FT-IR spectrum of THCB showed in Fig. 2c. Absorption peaks at around of 3270 cm^{-1} and 1550–1649 cm^{-1} were related to the stretching vibration and bending vibration of N—H group, respectively. Furthermore, the bands at around 3415 cm^{-1} and 1218 cm^{-1} could be attributed to the stretching vibration of the O—H and C—O in the phenol group. On the other hand, the absorption bands in the 1708 cm^{-1} and 663–749 cm^{-1} region were assigned to the stretching of the carboxylic acid C═O group and the swing vibration of C—Br in THCB.

Modification of alumina

The polar functional groups in the backbone of THCB can interact with the hydrophilic surface of inorganic materials via hydrogen bonding and electrostatic interaction as a monolayer. These chains, through of steric hindrance and interparticle electrostatic repulsion were prevented further coalescence in ANPs (Fig. 1). For getting good dispersion of the ANPs in the polymer matrix and control the size distribution, we applied the ultrasonic device. It is expected that the aggregation of ANPs can be broken down by generating local conditions of extremely high temperatures and pressures, which were produced by ultrasonic huge shock wave in a solution.

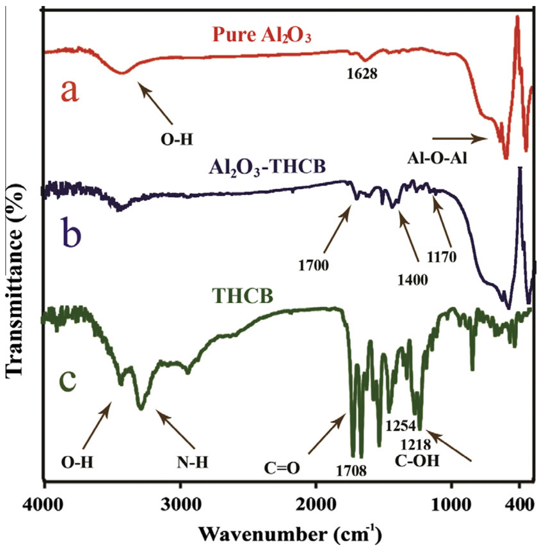

Fig. 2. FT-IR spectra of (a) pure ANP, (b) ANP/THCB, (c) THCB.

The FT-IR spectra using KBr of the pure ANP and modified ANP was shown in Fig. 2a and b. In the pristine alumina the broad absorption band at 3300–3400 cm^{-1} and weak band at 1628 cm^{-1} can be caused by stretching vibration and bending vibration of hydroxyl group peaks on the ANPs surface. Moreover, peak appeared in the vicinity of 400–1000 cm^{-1} is related to characteristic of absorption band of α-Al_2O_3. After modification of ANP with THCB (Fig. 2b), presence of a broad band in the 3500–3300 cm^{-1} region could be due to the stretching vibrations of O—H or N—H groups with varying degrees of H-bonding. The appearance of the new absorption peaks at 1170, 1266 cm^{-1}, and

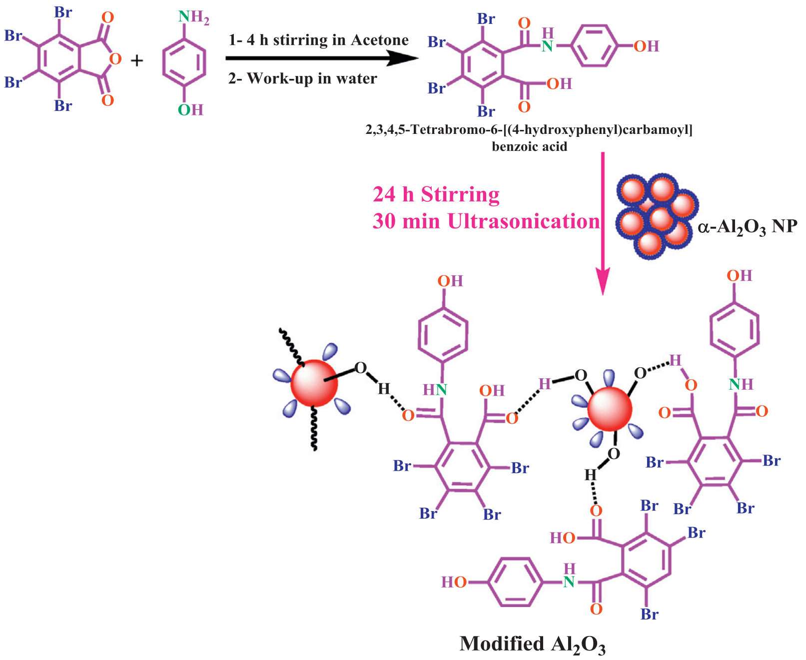

Fig. 1. Synthesis of the THCB as a modifier and preparation of the modified Al_2O_3.

1127 cm^{-1} (stretching vibration of the C—O group) and small peak at 1400 cm^{-1} (C—O—H deformation vibrations) are confirmed the presence of THCB onto the ANPs surface.

Synthesis of monomer and polymer

DAPh monomer was obtained by the condensation reaction of an equimolecular amount of TMA and L-phenylalanine amino acid in refluxing acetic acid solution at 120 °C, as shown in Fig. 3 [24].

Phosphorylation polymerization technique has been successfully applied to synthesize high molecular weight organosoluble PAI, which first was described by Yamazaki et al. [26]. In this paper, we used a simple, safe, and efficient method, without any use of carcinogenic organic solvents for the step-growth polymerization. In synthetic strategy, an equimolar amount of the DAPh and NDA monomers were mixed in the presence a molten ionic liquid (TBAB), which acted both as solvent and catalyst in conjunction with TPP. The inherent viscosity of the synthesized PAI under optimized condensation was 0.18 dL g^{-1} and the yield was 95%. The optical specific rotation of this polymer was $[\alpha]_D^{25} = +18.82°$ (0.05 g in 10 mL of DMF) [25].

In the FT-IR spectrum of the nanostructure PAI (Fig. 4a), absorption bands in 3300–3400 cm^{-1} (N—H stretching bands of the amide group), 3059 cm^{-1} (C—H aromatic), 2962 cm^{-1} and 2931 cm^{-1} (C—H aliphatic), 1777 cm^{-1} and 1719 cm^{-1} (imide C=O asymmetric and symmetric stretching), and 1671 (amide C=O stretching), are substantiated the polymer structure. Moreover, absorption peaks at 1381, 1171 and 729 cm^{-1}, shown the presence of the imide heterocycle ring in the PAI.

Synthesis of PANC

The synthesis of PANCs was carried out by insertion of ANPs into the polymer matrix via an ultrasonic irradiation process at ambient temperature. Due to the hot spots (high temperatures and pressures) which produce during sonication, the ANPs could be dispersed and combined with the PAI matrix. Different percentages of organically modified ANPs (5, 10, and 15 wt.%) were combined with the PAI matrix (Fig. 5). Surface modification of ANPs improved successfully the adhesion of polymer matrix to the surface of NPs. The THCB groups or remaining hydroxyl groups on the surface of ANPs can interact with the functional groups of PAI, like C=O and N—H via hydrogen bonding. Fig. 4b–d shows the FT-IR spectra of PANCs with various ratios of ANPs. Compared to the pure PAI, slight different positional displacement and new absorption bands around 400–1000 cm^{-1} in the FT-IR spectra of PANCs can be related to the formation of new interaction and hydrogen bonds between modified ANPs with the functional groups of PAI. For example, absorption peaks of carbonyl group from 1719 and 1671 cm^{-1} shifted towards 1725 and 1660 cm^{-1}, respectively which are related to the partial transfer of the electron pair in the functional groups of PAI.

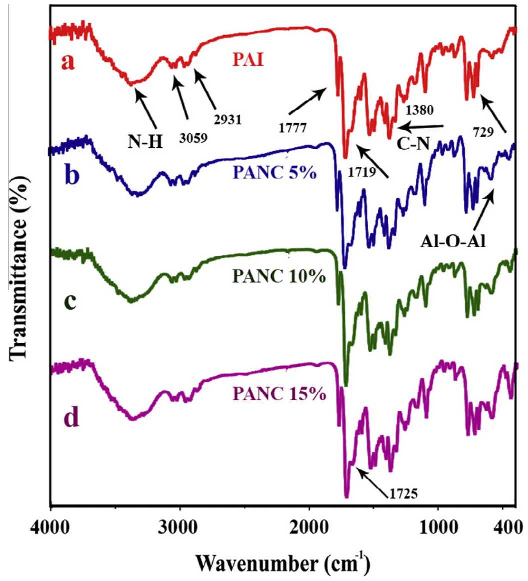

Fig. 4. FT-IR spectra of (a) pure PAI, (b) PANC5%, (c) PANC10%, (d) PANC15%.

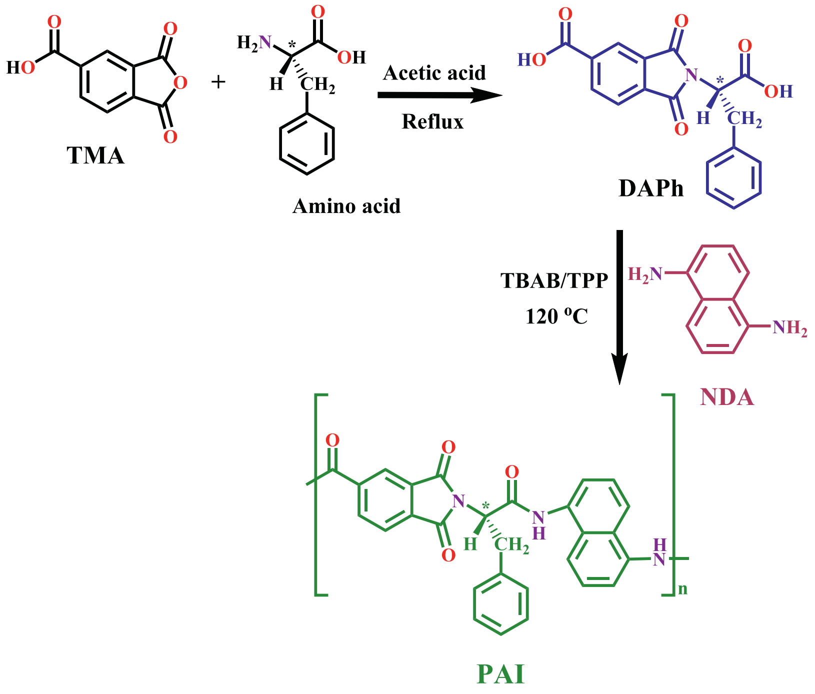

Fig. 3. Synthesis of DAPh (monomer) and PAI.

XRD

The XRD patterns of the PAI, PANCs and modified ANPs are shown in Fig. 6. The obtained diffractogram of PAI, obviously showed broad halo pattern without any obvious sharp peak demonstrating that the polymer was essentially amorphous. This amorphous nature is related to the presence of pendent groups, noncoplanar and twisted units, which reduce the backbone symmetry and regularity into the backbone of the obtained polymer. According to Fig. 6a, the XRD pattern of the modified ANP with THCB modifier indicated a good accordance with the reference XRD pattern of α-Al_2O_3 (42-1468 JCPDS file) and proved that the capping agent do not have any effect on crystallinity of ANPs. According to the XRD patterns of PANCs (Fig. 6b and c), after embedment of ANPs into the polymer matrix, the phase of ANPs has not been distorted during the sonication process. Of course, the intensity of ANP peaks turned into weaker in the presence of the host polymer, because of the ultrasonic irradiation by the production of many localized hot spots in the solution may decreased the crystallite size of α-Al_2O_3. The hexagonal structure of α-Al_2O_3 was confirmed by the diffraction peaks of (104), (113), and (116). The average crystalline size of ANPs in the PANC was determined from the half width of the diffraction using the Debye–Scherrer equation [27], which is approximately 17–22 nm.

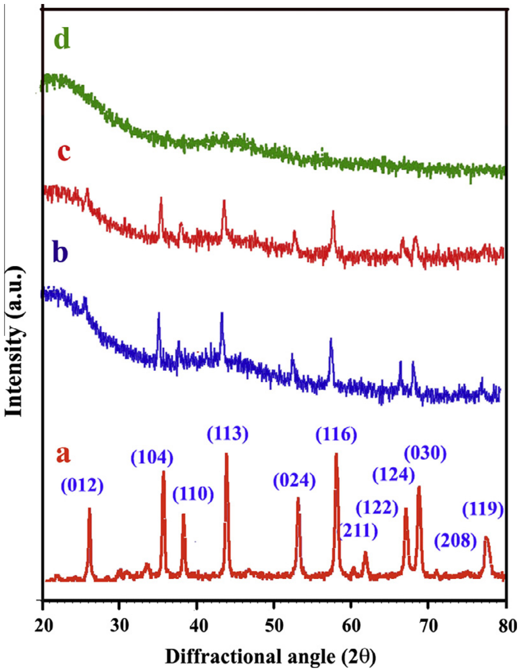

Fig. 6. XRD curves of (a) modified ANP, (b) PANC10%, (c) PANC15% and (d) pure PAI.

FE-SEM

The FE-SEM images of modified alumina, neat nanostructure of PAI and PANCs with magnification of 300 nm and particle size distribution histogram are shown in Fig. 7. The particle size distribution for modified ANPs showed a narrow Gaussian curve with mean

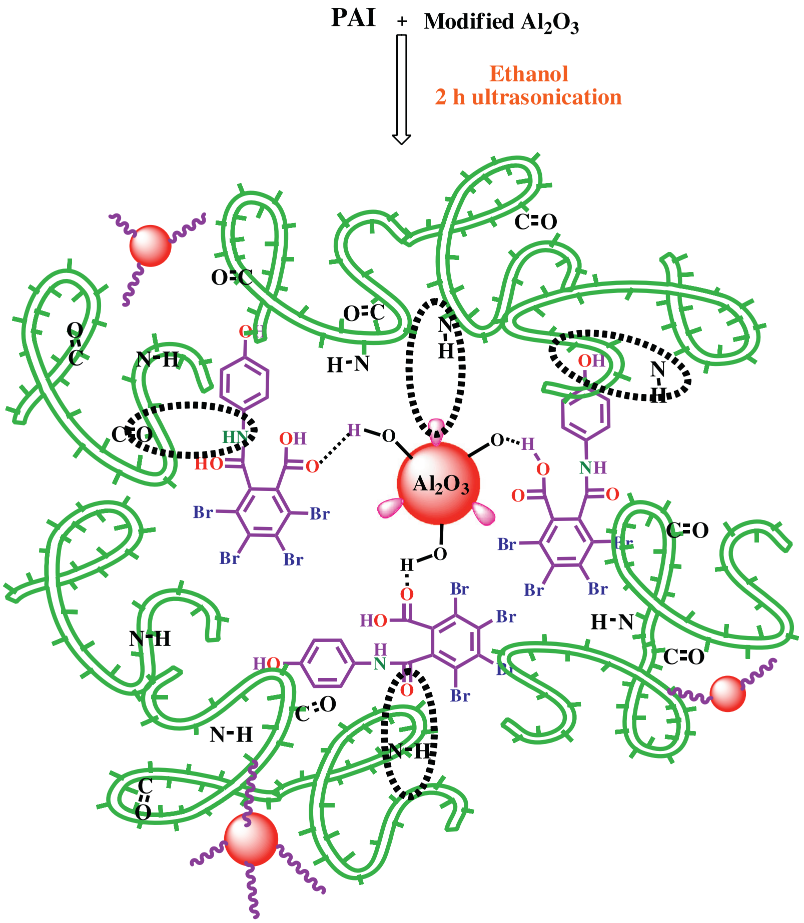

Fig. 5. Preparation of PANC and possible interactions (hydrogen bonding) between PAI and modified Al_2O_3.

size 23 ± 5 nm. Fracture surface micrograph of PAI (Fig. 7b) indicated that the average diameter of polymeric particles was about 25 ± 3 nm. In addition, means of particle size in PANCs 5, 10, and 15 wt.% with the narrow size distribution curves were established to be about 19, 21, and 22 ± 4 nm, respectively. These images and curves demonstrated that the ANPs were uniformly dispersed into the PAI matrix, also slightly agglomeration can be related to intermolecular interaction. The organic chains grafted on the surface of ANPs bring mutual exclusion and steric hindrance effect, thus the surface free energy has been reduced correspondingly and the agglomeration is controlled.

TEM

The formation of a true nanoscaled composite is further evidenced by using TEM analysis. This analysis, unlike of the FE-SEM analysis that is provided images from the samples surface, is employed to insights into the internal structure of different components. The TEM image, and the size distributions of the pure ANPs, modified ANP and PANCs are shown in Figs. 8 and 9. TEM micrograph of the pure ANPs (Fig. 8) exhibited particles with polyhedral morphology in the range of 60–90 nm [28]. Images of modified ANPs (Fig. 9a and b) have shown a broad size distribution, with minimum size NPs of about 10 nm and largest NPs with irregular shape and pumpkin in the size more than 50 nm. This particle size distribution probably is due to aggregation or clustering of NPs via hydrogen bondings (or could be due to arrangement of a few particles by hydrogen bonding which cannot resist the attraction with THCB). The representative TEM images of the PANC 10 wt.% with magnification of 30 and 40 nm are shown in Fig. 9c and d. It can be seen that the ANPs with spherical shapes and average particle diameter 18 ± 4 nm were dispersed in the polymer matrix. In PANCs, the particle sizes were believed to have been reduced; because of capping agents onto the NP surface could inhibit growth and agglomeration of NPs. Above and beyond, ultrasonic irradiation is a well-established method for particle size reduction in suspensions.

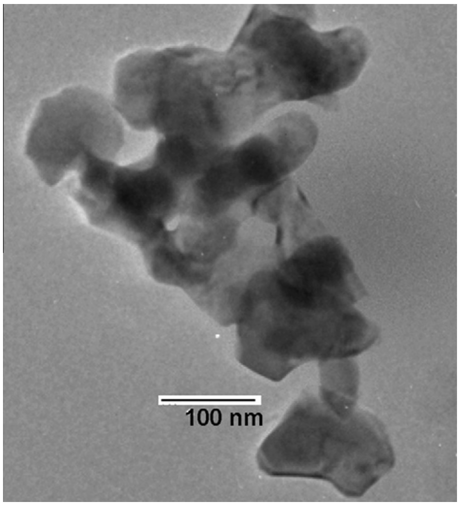

Fig. 8. TEM micrograph of pure ANPs [28].

Thermal properties investigation

TGA curves of the modified ANP, PAI and the PANCs are shown in Fig. 10. The thermal stability of the polymer and NCs were investigated by comparing the 5% and 10% weight losses (T_5 and T_{10}, respectively) of the samples and percent char yield at 800 °C. The curve of pristine ANP shows a small mass loss 3% in temperature range of 0–800 °C, which is related to the removal of the physically absorbed water [28]. In the thermogram of the modified ANP weight loss at around 270–800 °C is 18%, which is attributed the decomposition of the chemical combined water and functionalized organic moieties attached on the surface of ANPs. The thermal behavior data for the PAI and the PANCs are summarized in Table 1. The T_{10} of pure PAI and the PANCs appeared at 381, 427, 437, and 441 °C, respectively. The results showed that decomposition

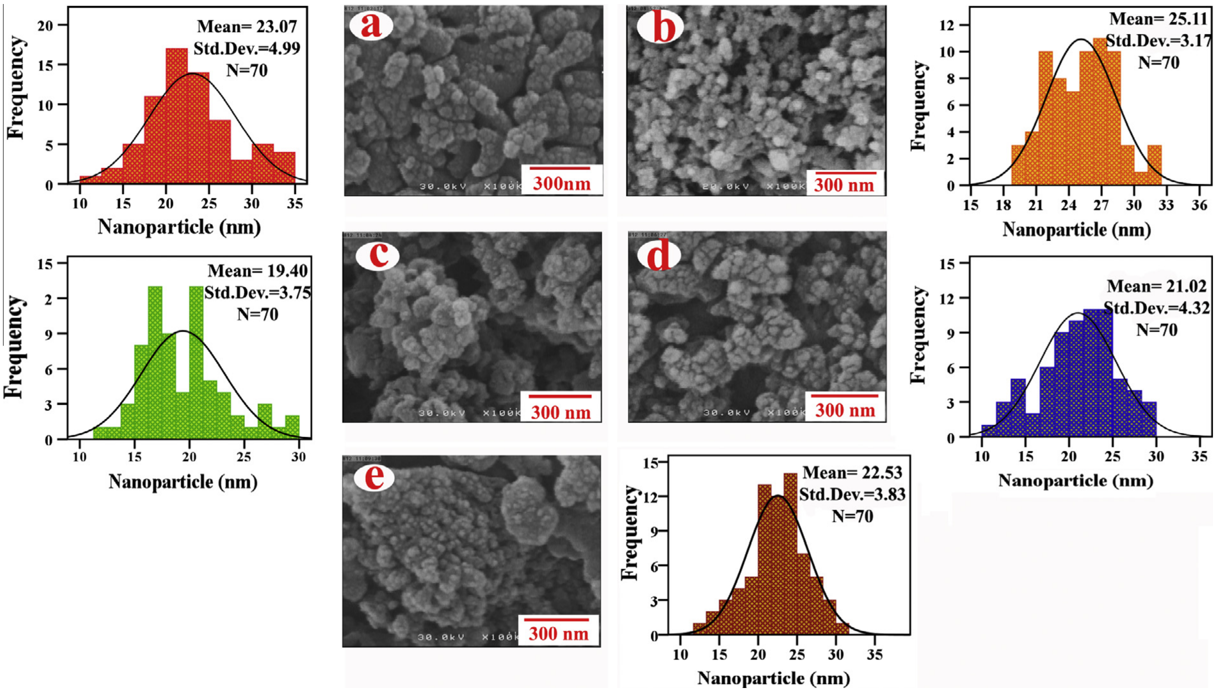

Fig. 7. FE-SEM micrographs and particle size distribution histograms of (a) modified ANPs, (b) pure PAI, (c) PANC5%, (d) PANC10% and (e) PANC15%.

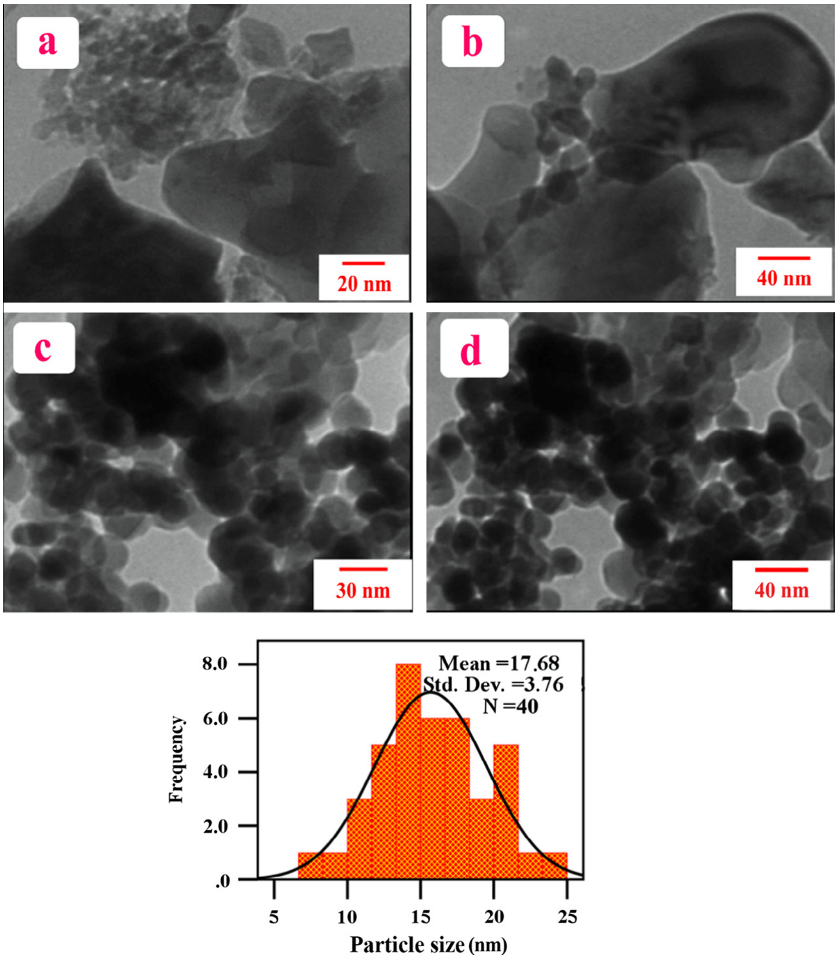

Fig. 9. TEM micrographs of modified ANP (a and b), PANC10% (c and d) and particle size distribution histogram of PANC10%.

temperature of PANCs shifted towards higher temperatures as the percentage of ANP was increased. The concentration of carbonized residue (char yield) of these composites in an argon atmosphere was more than 50% at 800 °C. The high char yield can be ascribed to their aromatic content and high heat resistance supplied by modified ANPs with flame retardant compound.

The limiting oxygen index (LOI) is a measure of the percentage of oxygen present to support the combustion of the material and can be used to assess the flame-retardancy of them.

$$\mathrm{LOI} = 17.5 + 0.4\,\mathrm{CR}$$

where CR = char yield.

According to Van Krevelen and Hoftyzer [29] there is a linear relationship between LOI and CR. From this equation, a higher char yield will increase flame retardancy. PAI and composites containing 5, 10, and 15 wt.% had LOI values 37, 38, 39, and 40, respectively, which were calculated from their char yield. On the basis of the LOI values, such materials were classified as self-extinguishing polymers and tend not to be burned.

Table 1
Thermal properties of the PAI and different PANC materials.

Sample	Decomposition temperature (°C)		Char yield (%)[b]	LOI[c]
	T_5[a]	T_{10}[a]		
PAI	352	381	49	37
PANC 5 wt.%	355	427	53	38
PANC 10 wt.%	369	437	54	39
PANC 15 wt.%	372	441	57	40

[a] Temperature at which 5% and 10% weight loss was recorded by TGA at the heating rate of 20 °C min^{-1} under argon atmosphere.
[b] Weight percentage of material left undecomposed after TGA analysis at a temperature of 800 °C under argon atmosphere.
[c] Limiting oxygen index (LOI) evaluated at char yield at 800 °C.

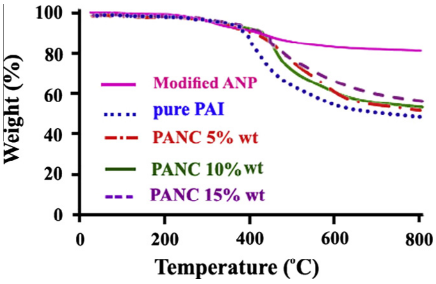

Fig. 10. TGA thermograms of modified ANPs, neat PAI and different PANC materials.

Conclusions

In this work, PANCs containing various ratios of the modified nano-ANPs with THCB were successfully synthesized using ultrasonic assistance method. Grafting of THCB on the surface of ANPs not only improved compatibility of ANPs in the polymer matrix, but also increased flame retardant property in the obtained PANCs.

The powerful ultrasonic irradiation was used as an effective and easy way for the one-step preparation of PANCs at ambient temperature. The superior energy of sonication process increased the probable interaction of the modified ANPs surface with different functional groups in the polymer backbone. The results of FT-IR spectra and XRD diffraction patterns proved that the ANPs existing in the host polymer and, also indicated that during the sonication process the structure of ANPs did not wrap. In the fracture surface micrographs of PANCs, the fillers were found well dispersion in the PAI matrix. The PANCs likewise, demonstrated improvement thermal stability when compared with the pure PAI. This enhancement in the thermal properties can be attributed to the high heat resistance exerted by ANPs and also, the absorption of flame retardant THCB on the ANPs surface.

Acknowledgments

This study was financially supported by the Research Affairs Division Isfahan University of Technology (IUT). Further financial support from National Elite Foundation (NEF), Center of Excellence in Sensors and Green Chemistry Research (IUT) is gratefully acknowledged.

References

[1] E. Abouzari-Lotf, A. Shockravi, A. Javadi, Polym. Degrad. Stab. 96 (2011) 1022.
[2] I. Bacosca, E. Hamciuc, M. Bruma, M. Ignat, React. Funct. Polym. 71 (2011) 905.
[3] S.-H. Hsiao, G.-S. Liou, Y.-C. Kung, Y.-J. Lee, Eur. Polym. J. 46 (2010) 1355.
[4] L. Chen, B.K. Goren, R. Ozisik, L.S. Schadler, Compos. Sci. Technol. 72 (2012) 190.
[5] Z. Lei, Y. Fan, Mater. Lett. 60 (2006) 2256.
[6] S.F. Motevalizadeh, M. Khoobi, M. Shabanian, Z. Asadgol, M.A. Faramarzi, A. Shafiee, Mater. Chem. Phys. 143 (2013) 1.
[7] B. Bittmann, F. Haupert, A.K. Schlarb, Ultrason. Sonochem. 18 (2011) 120.
[8] B.A. Rozenberga, R. Tenne, Prog. Polym. Sci. 33 (2008) 40.
[9] H. Ji, X. Liu, X. Wu, X. Wang, X. Hua, X. Yang, L. Lu, J. Mol. Struct. 935 (2009) 8.
[10] R.J. Kalbasi, M. Negahdari, J. Mol. Struct. 1063 (2014) 259.
[11] G.A.H. Mekhemer, A.K.H. Nohman, N.E. Fouad, H.A. Khalaf, Colloids Surf., A 161 (2000) 439.
[12] J. Li, Y. Pan, C. Xiang, Q. Ge, J. Guo, Ceram. Int. 32 (2006) 587.
[13] H. He, W. Jing, W. Xing, Y. Fan, Appl. Surf. Sci. 258 (2011) 1038.
[14] S. Kango, S. Kalia, A. Celli, J. Njuguna, Y. Habibi, R. Kumar, Prog. Polym. Sci. 38 (2013) 1232.
[15] J. Lin, H. Chen, Y. Yuan, Y. Ji, Appl. Surf. Sci. 257 (2011) 9024.
[16] P. Nordell, F. Nilsson, M.S. Hedenqvist, H. Hillborg, U.W. Gedde, Eur. Polym. J. 47 (2011) 2208.
[17] S. Mallakpour, M. Dinari, J. Macromol. Sci. Phys. 52 (2013) 1651.
[18] H. Li, Y. Yan, B. Liu, W. Chen, S. Chen, Powder Technol. 178 (2007) 203.
[19] E. Richard, S.T. Aruna, B.J. Basu, Appl. Surf. Sci. 258 (2012) 10199.
[20] E.M. Soliman, M.B. Saleh, S.A. Ahmed, Talanta 69 (2006) 55.
[21] K. Sato, H. Yılmaz, A. Ijuin, Y. Hotta, K. Watari, Appl. Surf. Sci. 258 (2012) 4011.
[22] A. Covaci, S. Voorspoels, L. Ramos, H. Neels, R. Blust, J. Chromatogr. A 1153 (2007) 145.
[23] S. Mallakpour, V. Behranvand, Colloid Polym. Sci. (2014), http://dx.doi.org/10.1007/s00396-014-3264-2.
[24] S. Mallakpour, S. Soltanian, M.R. Sabzalian, Colloid Polym. Sci. 289 (2011) 93.
[25] S. Mallakpour, E. Khadem, High Perform. Polym. (2013), http://dx.doi.org/10.1177/0954008313516820.
[26] N. Yamazaki, M. Matsumoto, F. Higashi, J. Polym. Sci., Part A: Polym. Chem. 13 (1975) 1373.
[27] N. Pimpha, S. Chaleawlert-umpon, P. Sunintaboon, Polymer 53 (2012) 2015.
[28] K. Laishram, R. Mann, N. Malhan, Ceram. Int. 38 (2012) 1703.
[29] D.W. Van Krevelen, P.J. Hoftyzer, Properties of polymers, third ed., Elsevier, New York, 1976.